ELSEVIER

Journal of Molecular Structure (Theochem) 546 (2001) 143–162

THEO CHEM

www.elsevier.com/locate/theochem

Cationic intermediates in *trans*- to *cis*- isomerization reactions of allylic systems. An exploratory ab initio study

Jenny C.Y. Yeung[a], Gregory A. Chasse[a,b,*], Edwin J. Frondozo[b], Ladislaus L. Torday[c,d], Julius G. Papp[c]

[a]*Department of Chemistry, University of Toronto, Toronto, Ont., Canada M5S 3H6*
[b]*Velocet Communications Inc., 210 Dundas St. W., Suite 800, Toronto, Ont., Canada M5G 2E8*
[c]*Department of Pharmacology and Pharmacotherapy, Albert Szent-Gyorgy Medical and Pharmaceutical Center, University of Szeged, H 6701 Szeged, Hungary*
[d]*Faculty of Medicine, University of Calgary, 3330 Hospital Drive N.W., Calgary, Alta, Canada T2N 4M1*

Received 20 December 2000; accepted 9 March 2001

Abstract

Computational analyzes were undertaken to investigate the geometrical isomerization mechanism of a truncated tail-end model (C_1–C_{10}) of the full lycopene molecule, the products of which are the 5-*cis* and 7-*cis*forms. The global conformational minima were identified for the neutral all-*trans* reactant, the cationic isomerization intermediates and that of these two *cis*-isomeric products. Energies and stabilities were compared during different stages of the isomerization mechanism of the segments. The C_4 allylic hydride affinity values of the all-*trans* to the 5-*cis*, and the 7-*cis* isomers of this lycopene model, are in the range of 255–260 kcal mol^{-1}, which are within the expected limits of such hydride affinity values (210 kcal mol^{-1} for weak and 360 kcal mol^{-1} for strong hydride affinity) at the RHF/3-21G level of theory. The bond lengths involving alternating single and double carbon–carbon bonds roughly coincide with the expected changes along each intermediate of the putative isomerization pathway. The following sequence of stability was observed in the tail-end model of neutral lycopene isomers:

5-*cis* > all-*trans* > 7-*cis*

For the cation, the order of stability was different:

all-*trans* > 5-*cis* > 7-*cis*

Keywords: Lycopene; Antioxidant; *trans*- to *cis*-isomerization; Carotenoids; Oxidative stress; Ab initio molecular orbital computations; 1,4-pentadiene; Tail-end model (C_1–C_{10}) of lycopene

* Corresponding author. Tel.: +1-416-598-3229; fax: +1-416-598-7797.
E-mail addresses: jenny.yeung@utoronto.ca (J.C. Yeung), gchasse@fixy.org (G.A. Chasse), efrondoz@velocet.ca (E.J. Frondozo), ltordai@ucalgary.ca (L.L. Torday), papp@phol.szote.u-szeged.hu (J.G. Papp).

0166-1280/01/$ - see front matter © 2001 Elsevier Science B.V. All rights reserved.
PII: S0166-1280(01)00441-9

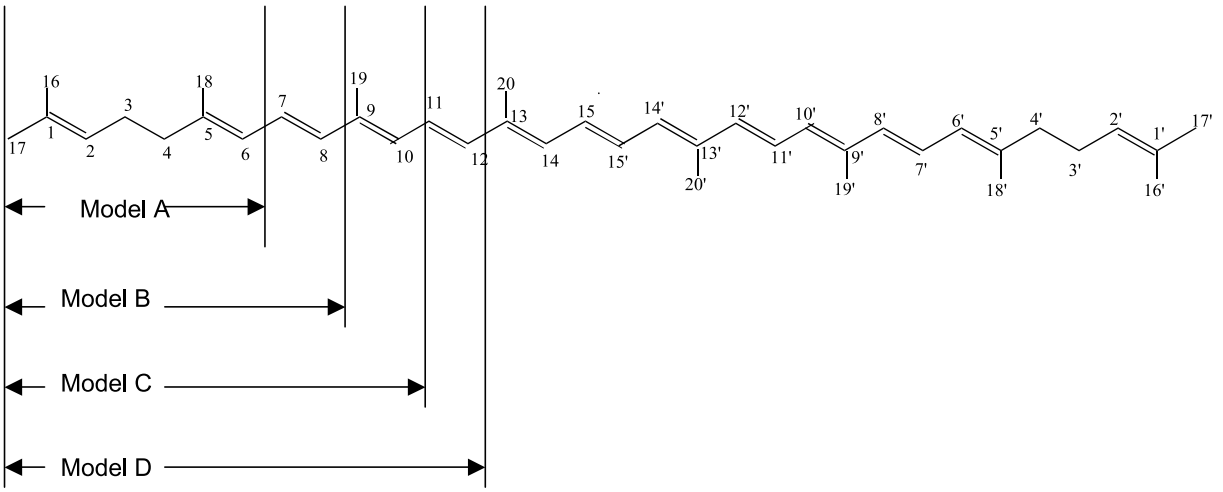

Fig. 1. Structure and numbering of lycopene and four experimental models.

1. Preamble

Lycopene (Fig. 1) belongs to a family of natural lipophillic pigments, known as carotenoids. Carotenoids, present in various fruits and vegetables, are fundamental constituents of plant photosystems. Perhaps the most extensively studied functions of carotenoids are their light-harvesting abilities during photosynthesis and protective effects against photosensitization, which could lead cancer. Today, approximately 700 carotenoids have been identified in nature [1], and their chemical structures have been unveiled. All carotenoids are characterized by an extended system of conjugated double bonds that account for their color and antioxidant activities. Carotenoids can be classified into hydrocarbon carotenoids containing solely carbons and hydrogens, and oxocarotenoids, which include oxygen atoms in their structure.

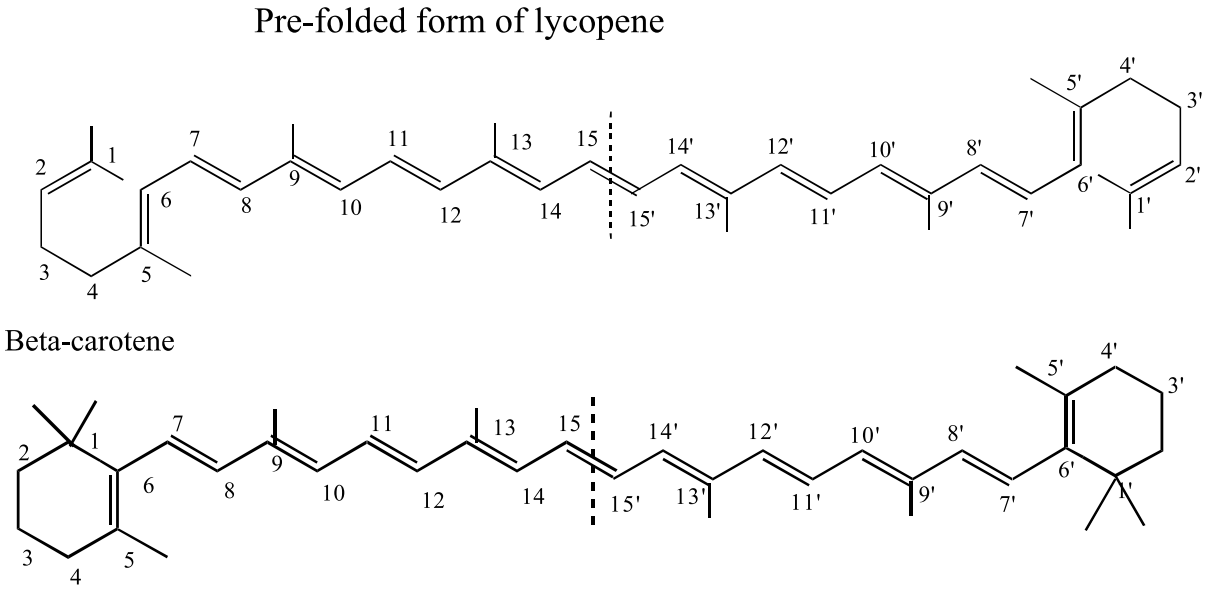

Fig. 2. Similarity in structure between lycopene (pre-folded) and beta-carotene.

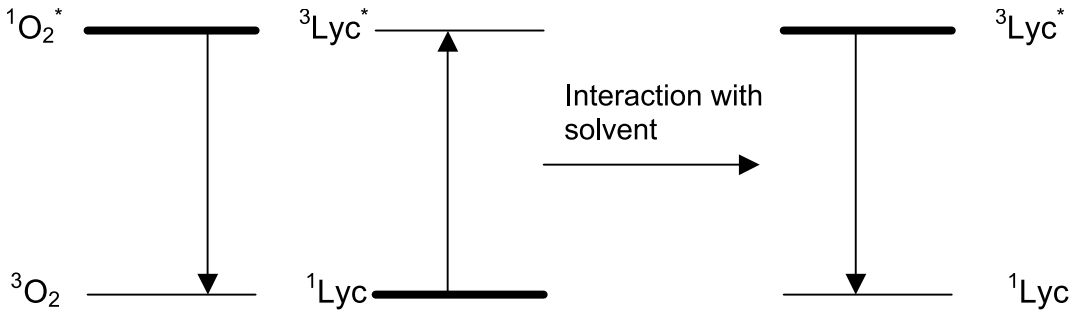

Fig. 3. Energy level diagram showing the energy transfer during $^1O_2$ scavenging (left side) the spin forbidden de-excitation of triplet lycopene (right side).

Another method of classification is based on the presence or absence of provitamin A activity. Originally, carotenoids were considered important only as precursors of vitamin A. More recently, there has been significant interest in evaluation of carotenoids for roles that are unrelated to their conversion to vitamin A. Beta-carotene has been the primary research focus of earlier studies because of its role in cancer prevention and its potential vitamin A activity. Although both lycopene and beta-carotene have very similar chemical structures (Fig. 2), and the former is even the precursor of the latter in the bio-synthetic pathway [2], the effects of lycopene and beta-carotene on health differ drastically. It is only recently discovered that instead of protecting humans against cancer, the supplement form of beta-carotene, when ingested, can increase the risk of lung cancer and heart disease [3]. Thus, the relationship between molecular structure and health is clearly demonstrated – even a diminutive difference in chemical structure can lead to unpredictable effects on health.

Although used as a natural food colorant for many years, it was only recently that lycopene became the subject of intense study with respect to its antioxidant activity and potential in alleviating chronic diseases such as prostate cancer [4]. A growing body of scientific evidence indicates that antioxidants are important in the human body's defences against harmful free radicals, which induce structural damages to cells and possibly contribute to aging and diseases that occur more frequently with advancing age. Lycopene, an antioxidant in vivo, provides protection against the oxidation of lipids, proteins and DNA by free radicals. The collective degenerative effects of these free radicals are termed 'oxidative stress'.

In fact, the most dangerous free radicals come from oxygen, known as the reactive oxygen species. They include superoxide (O_2^-), hydrogen peroxide (H_2O_2), hydroxyl radicals ($\cdot OH$) and singlet oxygen ($^1O_2$). Singlet oxygen is a very high energy form of oxygen with a shorter life than an oxygen radical, but damage cells and tissues much more quickly. Lycopene may well be the most potent of all singlet oxygen quenchers. Its efficiency for radical quenching resides in its extended system of conjugated double bonds. The greater the number of conjugated double bonds, the higher the ability of a carotenoid to quench free radicals [5]. Lycopene antioxidant activity begins with the transfer of energy of singlet oxygen to the carotenoid, yielding a triplet ground state oxygen and

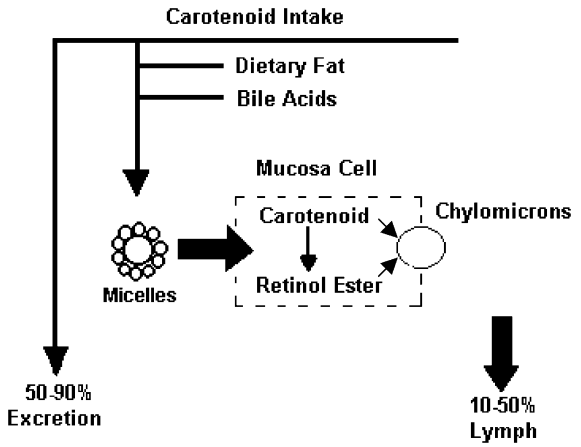

Fig. 4. Absorption of carotenoids (lymphatic pathway).

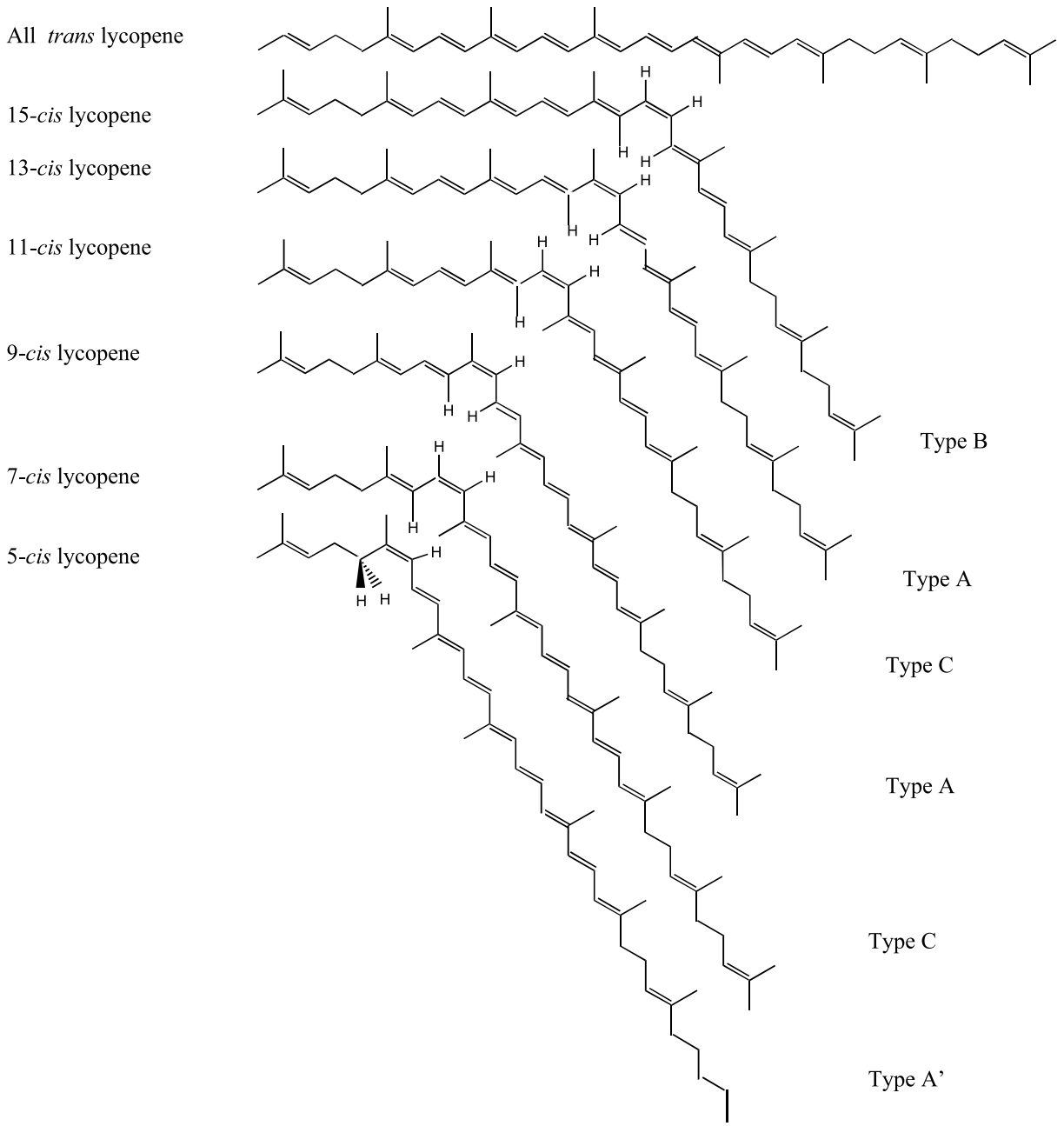

Fig. 5. Geometrical isomers of lycopene.

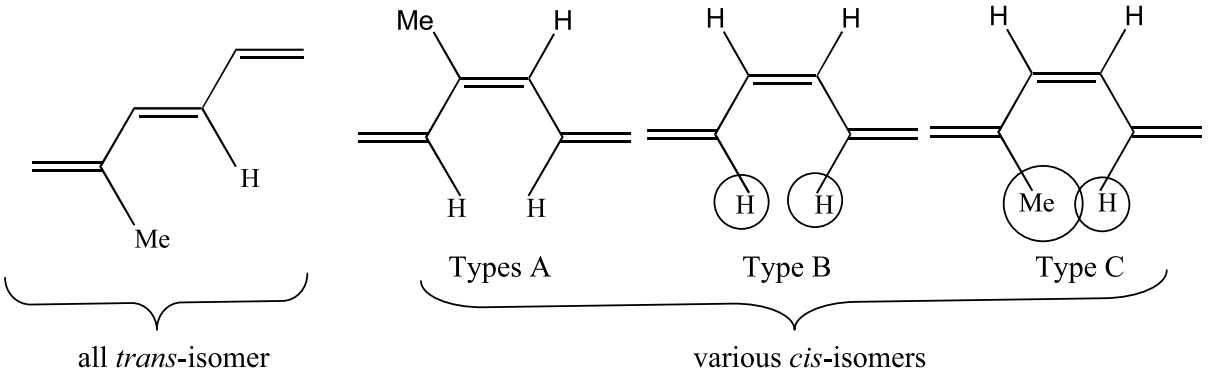

Fig. 6. Interaction between a methyl group and hydrogen group in lycopene.

a triplet-excited carotenoid (Fig. 3). Subsequently, the carotenoid returns to ground state by dissipating its energy through interaction with the surrounding solvent [6]. In fact, lycopene acts like a catalyst since it is left intact in this quenching process; also, once its job is finished, the physical quenching process begins again when lycopene further quench another singlet oxygen molecule. Furthermore, lycopene may also undergo isomerization during quenching, via the lowest triplet state of the molecule [5].

Together with dietary lipids and bile acids, lycopenes are incorporated into lipid micelles in the small intestine via the lymphatic pathway when it is taken into the body (Fig. 4). It is possible that configurations of different lycopene isomeric forms determine the ease of micelle formation, thus, aiding absorption of carotenoids into the intestinal mucosa cell. However, whether an in vivo isomerization mechanism exists is still unknown. The intact carotenoid is subsequently incorporated into chylomicrons, which are released into the lymphatic system for transport to the liver. The highest levels of lycopene have been found in the testes, adrenal glands and prostate [7]. The bioavailability of lycopene after its absorption and distribution in the body depends on various factors: food processing and presence of dietary lipids. Interestingly, processing such as heating has traditionally been considered as contributing towards the loss of nutritional quality of foods. In contrast, research confirmed that processing breaks down cell walls, which weakens the bonding forces between lycopene and tissue matrix, thus making lycopene more easily absorbed. Isomerization occurs during processing, converting a portion of the all-*trans* isomers to a mixture of *cis*-isomers. Lastly, since lycopene is a fat-soluble substance, it must be consumed with some fat in order to be absorbed through the intestine to achieve best results.

2. Introduction

2.1. Structural background

Lycopene has a chemical formula of $C_{40}H_{56}$. It is an acyclic and internally symmetrical molecule with 11 conjugated double bonds. Zechmeister [8] pointed out the possible existence of 72 geometrical isomers of lycopene. However, the most predominant species in tomatoes and tomato products is the all-*trans* isomer. Lycopene is present naturally in human plasma as an isomeric mixture containing over 60% of the total lycopene as *cis* isomers [7].

The all-*trans*, 5-*cis*, 9-*cis*, 13-*cis*, and 15-*cis* lycopene (Fig. 5) are commonly identified in human serum. Not all *cis*-isomers are of equal stability due to a number of possible 1,4 interactions between neighbouring methyl and hydrogen groups (Fig. 6). Pauling called attention to the fact that *trans*- to *cis*-isomerization can be a result of overlapping of the methyl group of a carbon atom adjacent to a double bond and the hydrogen [9]. Apparently, the steric interaction between a methyl group and hydrogen atom (Fig. 6) is the most destabilizing which is based on their relative group sizes.

2.2. Computational background

Conformational analysis has been performed on a truncated (C_1–C_8) tail-end model (see Model B in Figs. 1 and 8) of lycopene [10]. The global minimum on the conformational Potential Energy Hyper-Surface (PEHS): $E = E(\chi 2, \chi 3, \chi 4)$, corresponds to the ($g^+$, a, g^+) structure, or its degenerate pair (g^-, a, g^-), for both the all-*trans* and 5-*cis* isomers. For the full lycopene isomers, the sequence of stability:

5-*cis* > all-*trans* > 9-*cis* > 13-*cis* > 15-*cis* > 7-*cis* > 11-*cis*

has been observed from previous ab initio calculations [11]. Apparently, the 5-*cis* form is the energetically most stable of all isomers not only in the case of the full lycopene, but also its truncated tail-end model (Model B) [10].

2.3. Scope

The aim of the present research is to study the isomerization mechanism (Fig. 7) of a truncated (C_1–C_{10}) tail-end model (Model C) of the full lycopene (Figs. 1 and 8), the products of which are two *cis* forms (5-*cis* and 7-*cis*). The use of this truncated tail-end model, which is considerably smaller than the full lycopene, permits more convenient and manageable molecular computations as well as a detailed examination of the two terminal portions of lycopene (from C_1 to C_5 and from C'_1 to C'_5) that rotate out of plane. Previous studies concluded [10,11] that lycopene has a rigid central skeleton (from C_5 toC'_5) and two flexible tails (from C_1 to C_5 and from C'_1 to C'_5).

As it can be seen from the proposed mechanism (Fig. 7), the cation formation converts C_4 from its nearly tetrahedral (sp^3), to a trigonal planar (sp^2) geometry. Since the positive charge is dispersed throughout the π-network, C_3 now has two trigonal planar carbons attached.

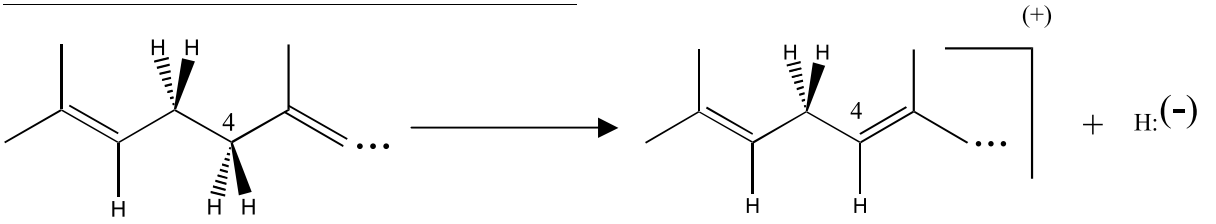

For this reason, it became necessary to study the conformational pattern of divinyl methane (1,4-pentadiene), before the cationic intermediates were investigated.

3. Methods

Completely relaxed geometric optimizations were performed at RHF/3-21G level of theory for the neutral all-*trans* as well as the 5-*cis* and 7-*cis* isomers, of lycopene Model C (Fig. 8) using the conformational information of Model B, published earlier [10]. The three cationic intermediates (i.e. the all-*trans*, the 5-*cis* and 7-*cis* form) were also subjected to the same analysis.

An ab initio (RHF/3-21G) 2D-scan was carried out to generate the $E = E(\phi, \psi)$ potential energy surface of divinyl methane, where ϕ and ψ represent rotations about the C(sp^2)–C(sp^3) and C(sp^3)–C(sp^2) single bonds, respectively. The visually observed minima were subjected to geometry optimizations at the RHF/3-21G level of theory. The results were used in studying the cationic reaction intermediates. GAUSSIAN 94 has been used to carry out all the computations [12].

4. Results and discussion

4.1. Conformations of divinyl methane

Divinyl methane (1,4-pentadiene) has been studied first, as a conformational model of the cationic intermediates. The essential question here is whether the two unsaturated moieties, joined to the central CH_2 unit, are coplanar or not. In other words, do minima

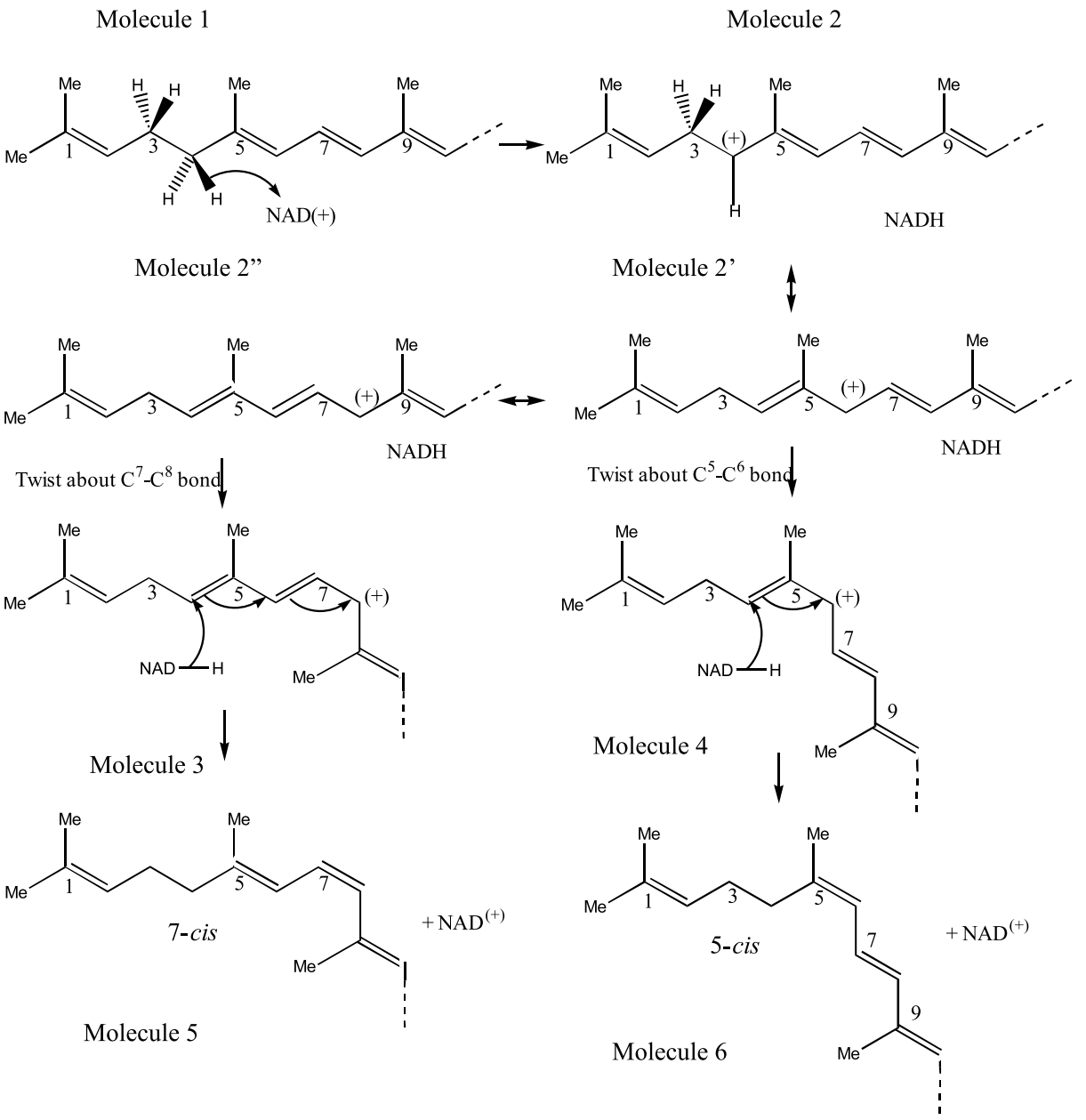

Fig. 7. Putative mechanism for lycopene isomerization.

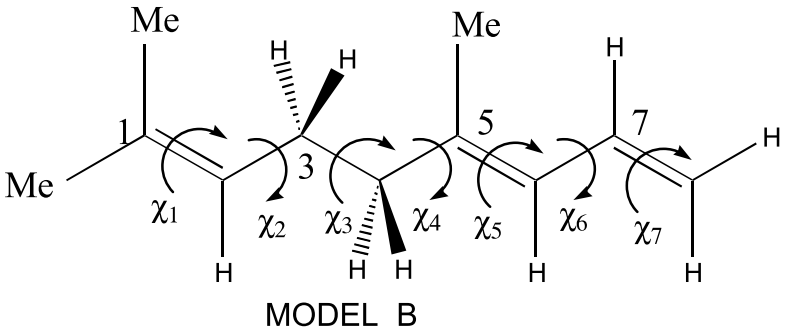

X_1: Me-C_1-C_2-C_3
X_2: C_1-C_2-C_3-C_4
X_3: C_2-C_3-C_4-C_5
X_4: C_3-C_4-C_5-C_6
X_5: C_4-C_5-C_6-C_7
X_6: C_5-C_6-C_7-C_8
X_7: C_6-C_7-C_8-H

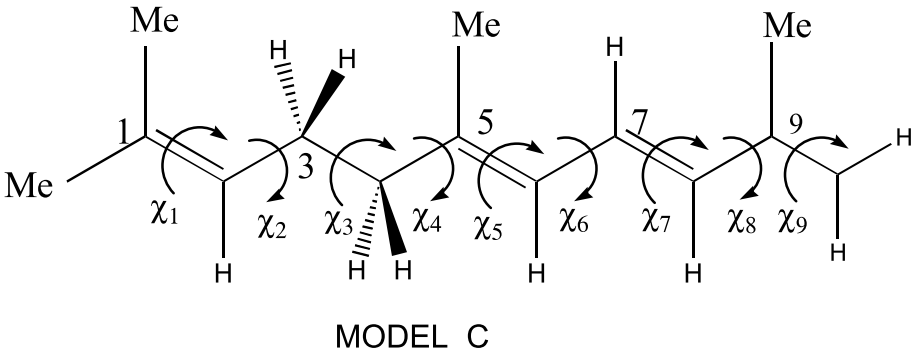

X_1: Me-C_1-C_2-C_3
X_2: C_1-C_2-C_3-C_4
X_3: C_2-C_3-C_4-C_5
X_4: C_3-C_4-C_5-C_6
X_5: C_4-C_5-C_6-C_7
X_6: C_5-C_6-C_7-C_8
X_7: C_6-C_7-C_8-C_9
X_8: C_7-C_8-C_9-C_{10}
X_9: C_8-C_9-C_{10}-H

Fig. 8. Structure and numbering of the tail-end models of lycopene. Model B includes the first eight carbons of lycopene's carbon backbone. Model C includes the first ten carbons of lycopene's carbon backbone.

occur either in the *syn*/*syn*, *syn*/*anti*, or in the *anti*/*anti* form.

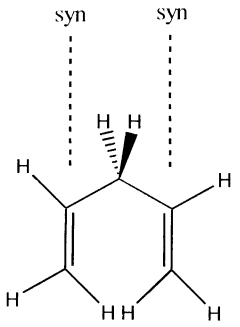

$(0^0, 0^0)$

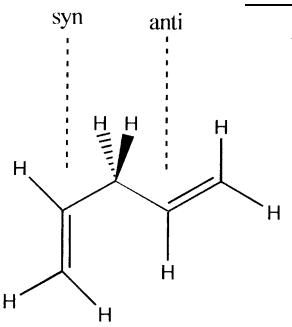

$(0^0, 180^0)$

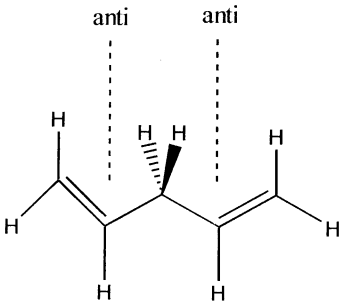

$(180^0, 180^0)$

The conformational PEHS of divinyl methane is shown in Fig. 9. The eight minima located were optimized and the results are summarized in Table 1.

The minima occurred in the vicinity of ±16 and ±120°. That means that the unsaturated moieties are either nearly perpendicular (corresponding to ±30°) to one or the other of the C–H bonds, or in alignment, i.e. eclipsed, (±120°) with one or the other of the C–H bonds. However, no minimum was observed at 0 or ±90°, when the olifinic groups would be eclipsed with or perpendicular to the C–C bond.

Torsional potential energy curves (PECs) of the type

$$E = E(\psi),$$

were generated at $\phi = 0°$ as well as $\phi = 120°$ and $\phi = -120°$, to see the alternation of minima and maxima along the torsional mode of motion. The results are shown in Fig. 10A and B, respectively.

4.2. Structures and stabilities, along the isomerization mechanism pathway of lycopene Model C

The *trans–cis* isomerization mechanism (Fig. 7) of Model C (Fig. 8B), as well as the conformational torsional angles and relative energies of its intermediates have been examined in detail. The geometries, energies and stabilities of all species involved are presented in Table 2.

Results obtained here for the neutral compounds are expected to follow the sequence of energy and stability of the full lycopene. The observed order of stability is clearly in agreement with earlier results obtained in the case of full lycopene [11]:

5-*cis* > all-*trans* > 7-*cis*

For the cationic intermediates, however, the order of stability is different:

all-*trans* > 5-*cis* > 7-*cis*

Table 1
Optimized dihedral angles, bond lengths, total energies and relative energies of various conformers of divinyl methane

Conformer	ϕ	ψ	C_3–H_9	C_3–H_{10}	Energy	ΔE (kcal mol^{-1})
a	116.85982686	116.8582153	1.08566470	1.08566516	−192.8732017	0.00000
a′	−116.86066755	−116.85996391	1.08566521	1.08566492	−192.8732017	0.00000
b	119.87843183	−119.87227647	1.08815294	1.08353286	−192.8718829	0.82756
b′	−119.87318394	119.87789676	1.08353187	1.08815307	−192.8718829	0.82756
c	16.10175702	−115.86964444	1.08760599	1.08673326	−192.8720363	0.73130
c′	−16.10317418	115.87135594	1.08673431	1.08760496	−192.8720363	0.73130
d	−115.86972268	16.1032023	1.08673701	1.0875990	−192.8720363	0.73130
d′	115.86753178	−16.10561373	1.08759825	1.08673763	−192.8720363	0.73130

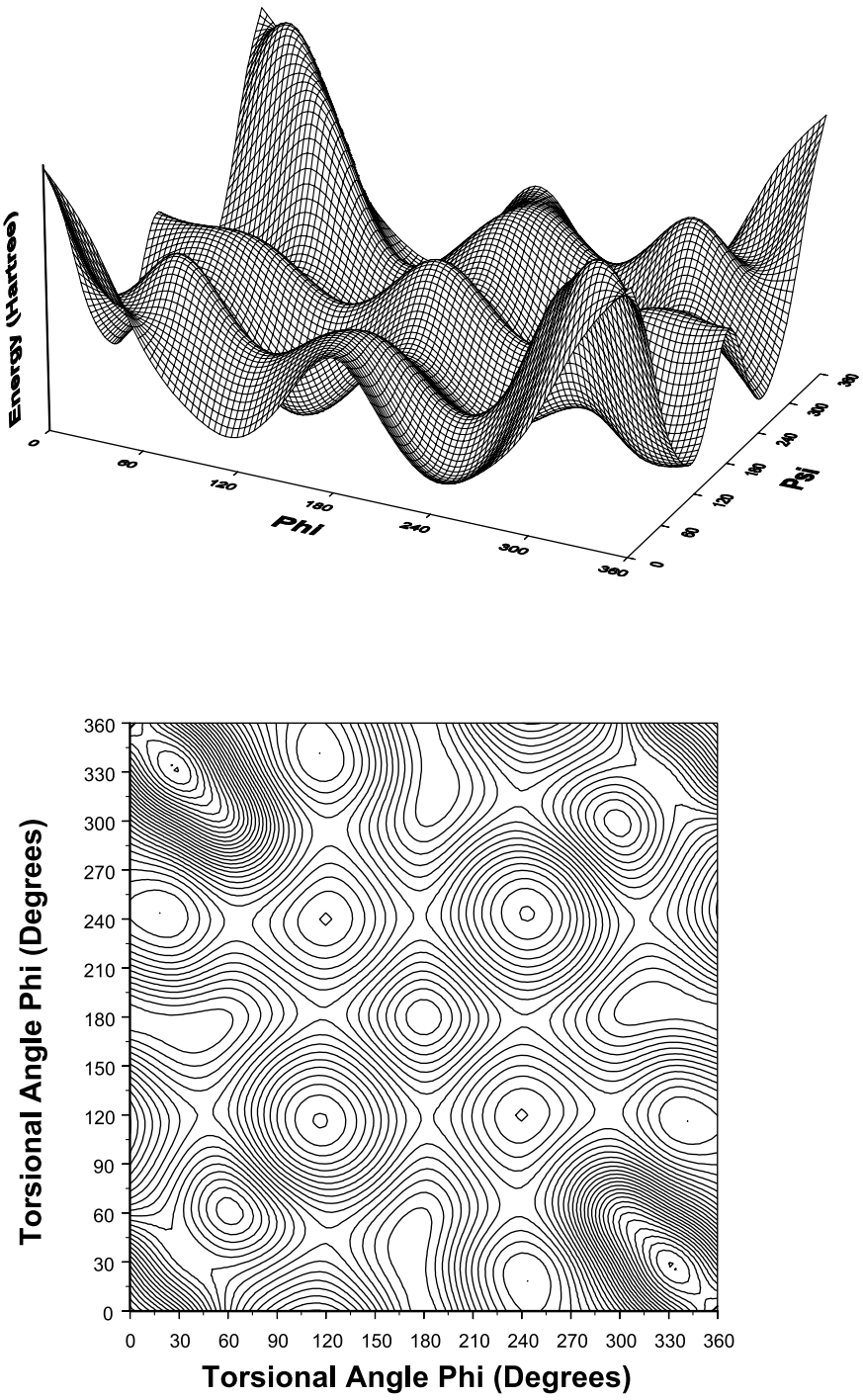

Fig. 9. Conformational potential energy surface of divinylmethane; $H_2C{=}CH{-}CH_2{-}CH{=}CH_2$; $E = E(\phi, \psi)$ where ϕ and ψ are the rotations about the two single bonds. Top: Landscape; Bottom: Contour representation.

The rotation PEC along ψ, of divinyl methane is structurally analogous to the rotational potential along χ_3 in the cationic intermediates of Model C. For the three cationic intermediates (i.e. for the all-*trans*, the 5-*cis* and 7-*cis* cations), the

$$E = E(\chi_3).$$

PECs are shown in Fig. 11. It is interesting to note that the cationic intermediates show a somewhat different torsional potential (Fig. 11) with respect to that obtained in the case of divinylmethane (Fig. 10). Although the increased size of Model C may be a factor, nevertheless it is more likely that the presence of the positive charge redistributes the electron density sufficiently, which in turn translates to a somewhat different conformational PECs.

4.3. Bond length interpretations

One of the structural features of the isomerization process is the changing carbon–carbon bond length. During the reaction, a double bond may change to a single bond and vice versa. Key bond lengths at various stages of isomerization are summarized in Table 3. The C–C single and C=C double bond lengths, obtained at this level of theory, are given, for the sake of comparison, in the footnote of Table 3.

Three types of CC bond lengths were identified:

double bond (approximately: 1.32 Å),
conjugated single bond (approximately: 1.47 Å),
genuine single bond (approximately: 1.54 Å).

On the basis that, a conjugated stabilization pattern has emerged, which is shown in Scheme 1. The broken line –- passing through three bonds from C_5 to C_8 are neither genuine single or genuine double bonds. Thus rotations may occur relatively easily along the C_5–C_6 and C_7–C_8 bonds. The results (Table 3 and Scheme 1) roughly coincide with the expected changes, but they are somewhat different from conventional resonance hybrid representation (c.f. Structures 2, $2'$ and $2''$ in Fig. 7).

4.4. Energetics of isomerization mechanism

The rotational potential energy curves associated with the isomerization processes

All-*trans cation* → 5-*cis cation*

All-*trans cation* → 7-*cis cation*

are shown in Fig. 12. The barriers to interconversions are different for the two processes. The two PECs clearly indicate that the isomerization to the 5-*cis* cation is kinetically more favourable than that to the 7-*cis* cation. However, the cations have to be formed in the first place. Hydride transfer to $NAD^{(+)}$ may lead to the formation of allylic cations.

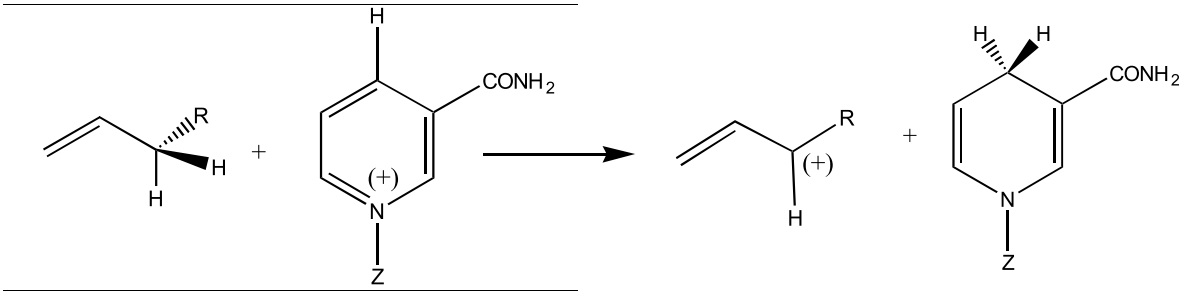

The relative ease of hydride [$H:^{(-)}$] removal is measured by the hydride affinity of the molecular system. Hydride affinity values, as computed at the RHF/3-21G level of theory, are summarized in Table 4. These data suggest that the easiest removal of an allylic hydride is from the all-*trans* isomer and the most difficult to remove, is from the 5-*cis* isomer. These results are illustrated graphically by Fig. 13, in the form which preserves the mechanistic considerations given in Fig. 7.

As far as the thermodynamics of the reaction are concerned, a great deal depends on the hydride affinity of the hydride acceptor. This is clearly shown in

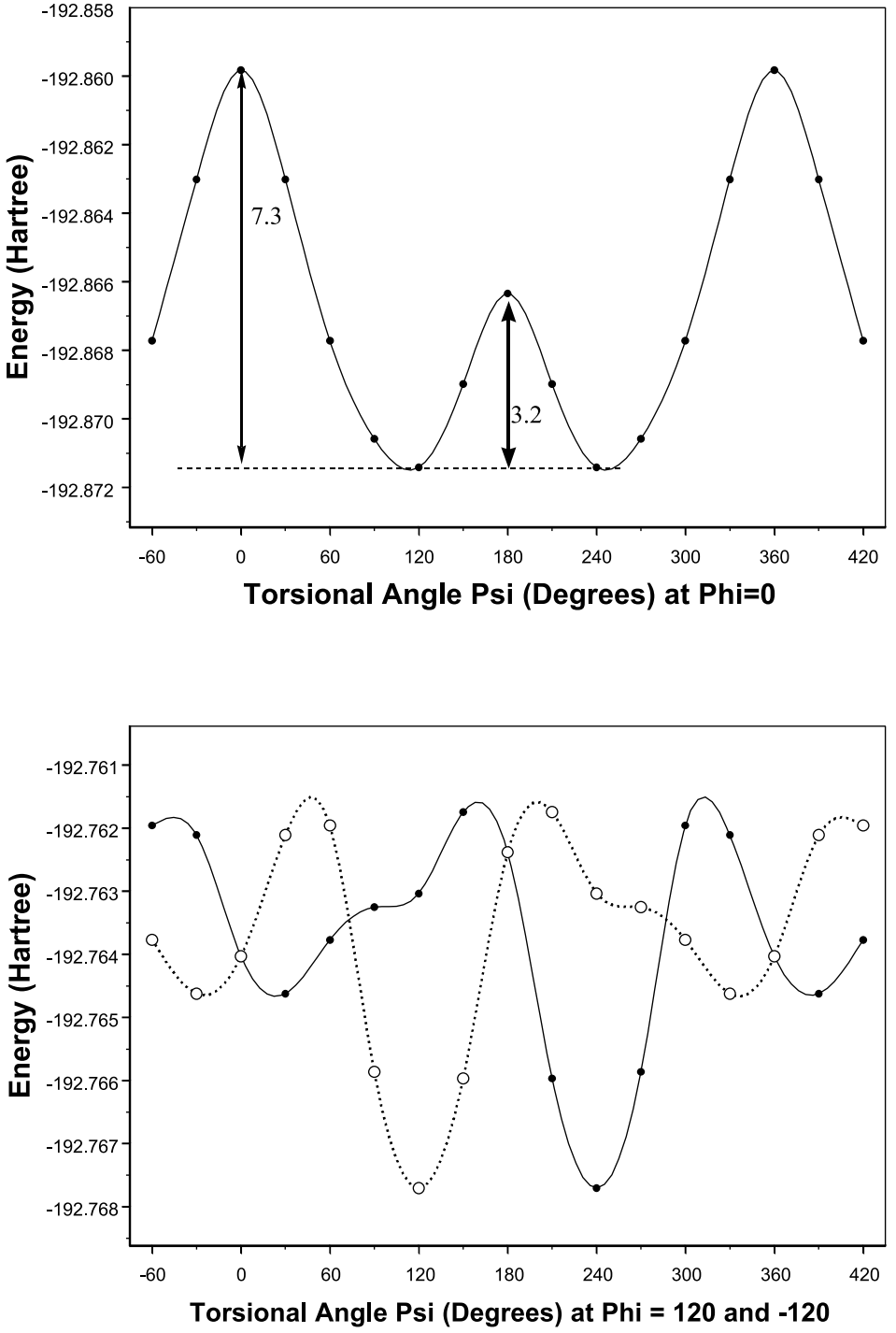

Fig. 10. Top(A): Torsional potential $E = E(\psi)$ at $\phi = 0°$, for divinylmethane. Bottom(B): Torsional potential $E = E(\psi)$ at $\phi = \pm 120°$, for divinylmethane.

Table 2
Torsional angles, total and relative energies for the reactant, intermediates and products of lycopene Model C isomerization

Isomer	Charge	χ_1	χ_2[a]	χ_3[a]	χ_4[a]	χ_5[b]	χ_6	χ_7[b]	χ_8	χ_9	χ_{10}[c]	χ_{11}[c]	χ_{12}[c]	Energy (Hartree)	ΔE (kcal mol^{-1})
All-trans	0	− 178.919	**106.090**	**176.414**	**100.211**	− 178.62	− 179.773	− 179.942	179.977	179.996	179.853	175.917	− 179.006	− 539.8927057	0.000000
5-*cis*	0	− 178.918	**103.058**	**176.448**	**90.186**	*1.362*	− 178.146	179.905	− 179.779	− 179.990	179.197	175.871	− 179.943	− 539.8933291	− 0.391190
7-*cis*	0	181.069	**106.427**	**176.351**	**99.600**	181.633	182.021	*0.772*	181.454	180.274	179.991	173.943	177.585	− 539.8833670	5.860127
>All-*trans*	+ 1	179.161	**97.958**	**99.284**	− 177.597	− 178.327	179.673	− 179.958	179.979	− 179.971	− 179.741	− 2.318	179.980	− 539.0853808	0.000000
5-*cis*	+ 1	179.030	**97.370**	**100.087**	− 177.362	*2.951*	− 179.406	180.000	− 0.003	− 0.001	− 179.933	− 178.288	179.894	− 539.0790704	3.959839
7-*cis*	+ 1	179.102	**98.443**	**98.994**	− 177.642	− 178.235	179.713	*0.098*	− 179.968	179.995	− 179.667	− 2.413	179.875	− 539.0750170	6.503388

[a] Conformational torsional angles, in bold.
[b] *cis*-isomeric torsional angles, in italics.
[c] Methyl rotations.

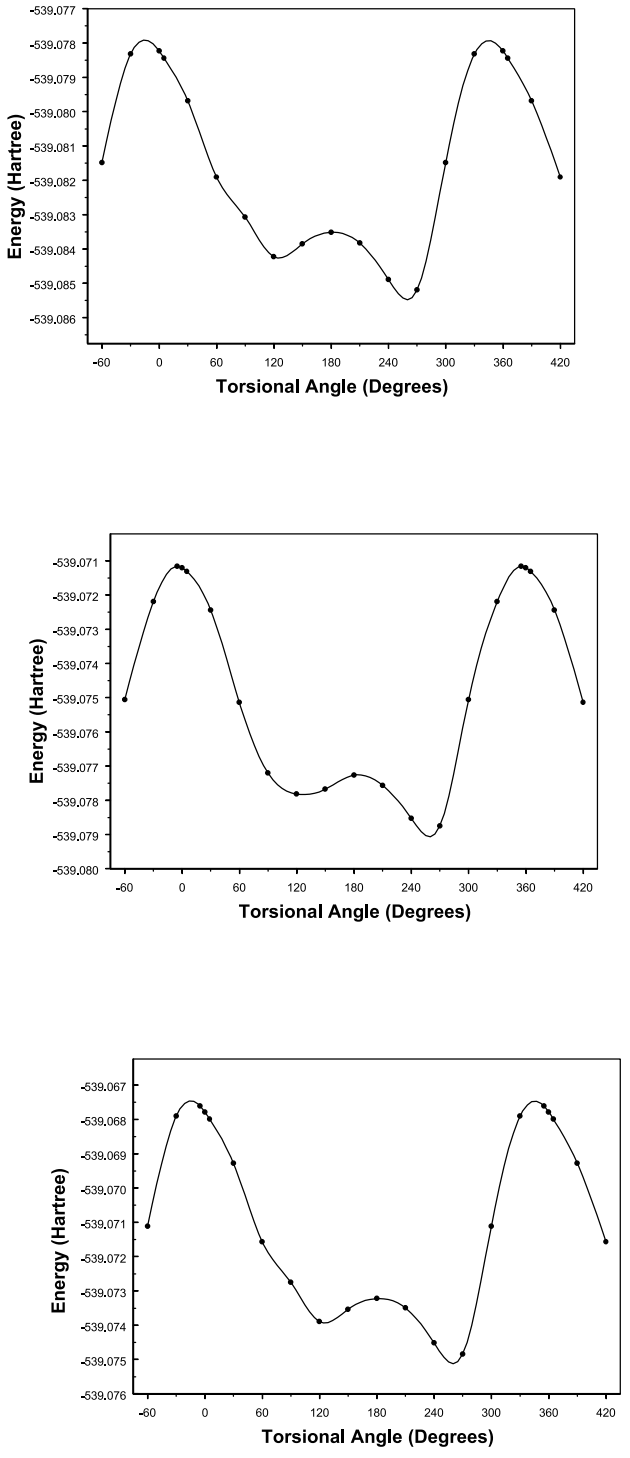

Fig. 11. Torsional potentials for the three cationic intermediates of lycopene Model C isomerization. Top: all-*trans*, middle: 5-*cis*, bottom: 7-*cis*.

all-trans

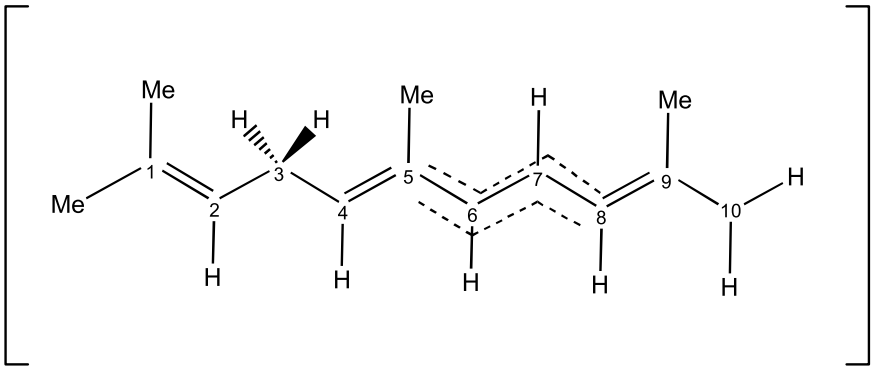

(+)

7-cis

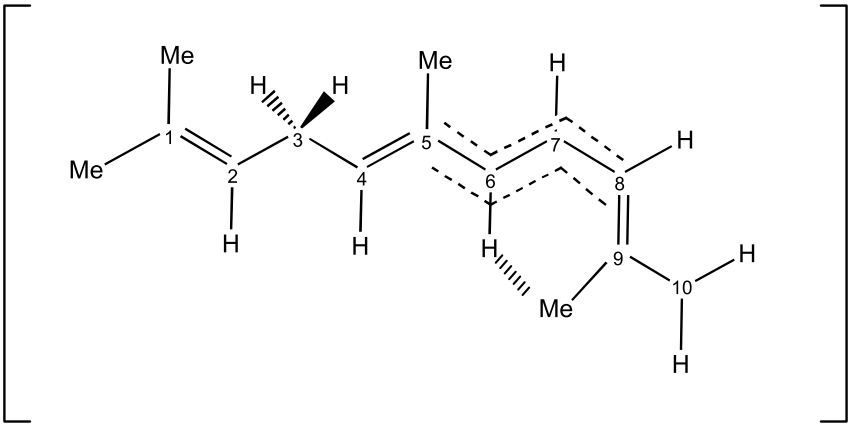

(+)

5-cis

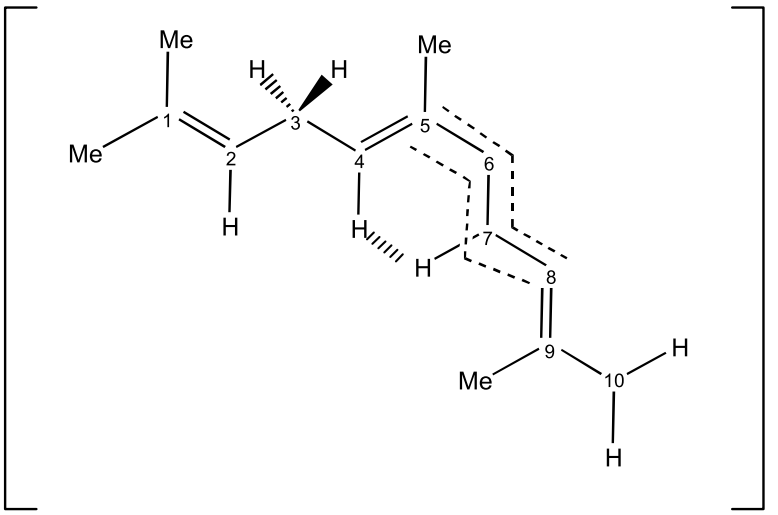

(+)

Scheme 1.

Table 3
Variation of carbon–carbon bond lengths along the isomerization pathway of lycopene Model C (conjugated single bonds in italic, double bonds in bold R[C–C] in ethane = 1.542, in butadiene = 1.467, R[C=C] in ethylene = 1.315, in butadiene = 1.320)

Molecule	Charge	R(Me-C_1)	R(C_1–C_2)	R(C_2–C_3)	R(C_3–C_4)	R(C_4–C_5)	R(C_5–C_6)	R(C_6–C_7)	R(C_7–C_8)	R(C_8–C_9)	R(C_9–C_{10})
All-*trans*	0	1.517	**1.321**	1.510	1.556	1.518	**1.328**	*1.462*	**1.328**	*1.472*	**1.325**
5-*cis*	0	1.517	**1.321**	1.510	1.556	1.517	**1.328**	*1.463*	**1.328**	*1.472*	**1.325**
7-*cis*	0	1.517	**1.321**	1.510	1.556	1.518	**1.329**	*1.463*	**1.332**	*1.478*	**1.326**
All-*trans*	1	1.516	**1.322**	1.529	1.495	**1.359**	*1.410*	*1.393*	*1.364*	**1.335**	1.516
5-*cis*	1	1.516	**1.323**	1.531	1.495	**1.358**	*1.412*	*1.399*	*1.362*	**1.334**	1.515
7-*cis*	1	1.516	**1.322**	1.529	1.495	**1.360**	*1.412*	*1.394*	*1.368*	**1.337**	1.516

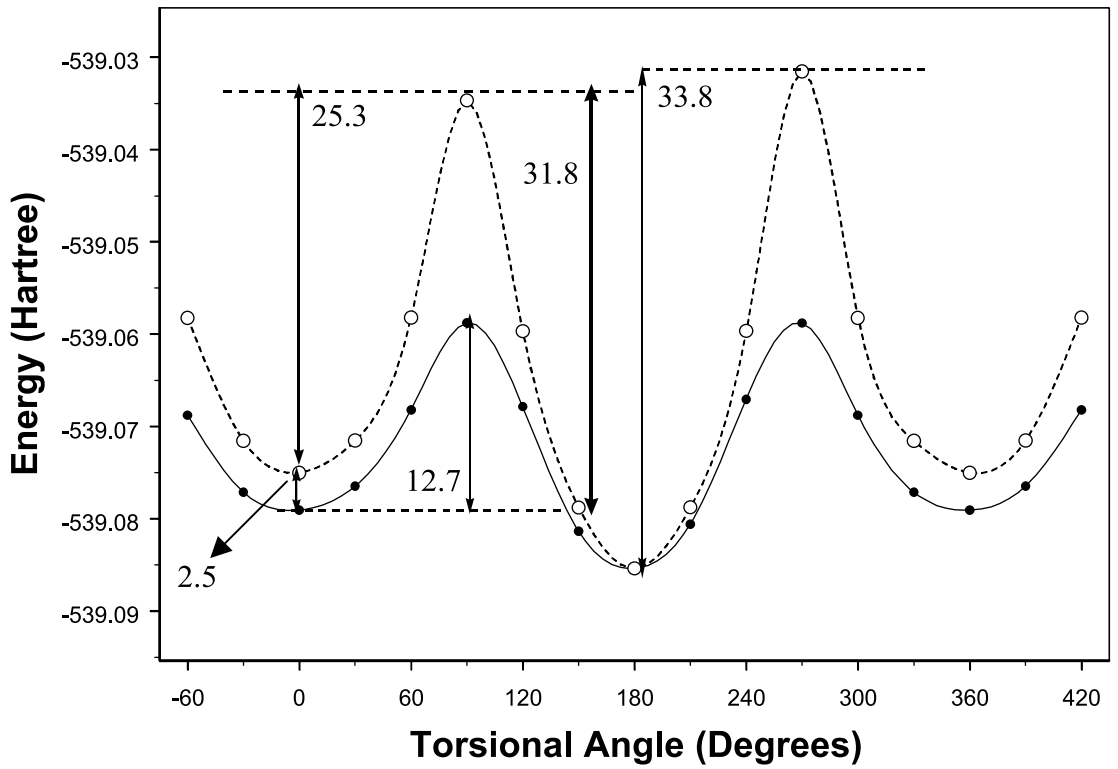

Fig. 12. Torsional potentials for the two isomerization processes Solid Line: all-*trans* → 5-*cis*, broken line: all-*trans* → 7-*cis*.

Table 4
Energy components ($E[H^{(-)}] = -0.4004207$ Hartree) for hydride affinities of selected compounds

Molecular system	Total energy (Hartree)		Hydride affinity (kcal mol^{-1})
	Cation	Neutral	
Weak hydride acceptor	−7.1870945 $Li^{(+)}$	−7.9298426 Li–H	214.813866774
Strong hydride acceptor	−39.0091291 $H_3C^{(+)}$	−39.9768768 H_3C–H	356.00336577
All-*trans* Model C	−539.0853808	−539.8927057	255.336454542
5-*cis* Model C	−539.0790704	−539.8933291	259.687483380
7-*cis* Model C	−539.0750170	−539.8833670	255.979715043

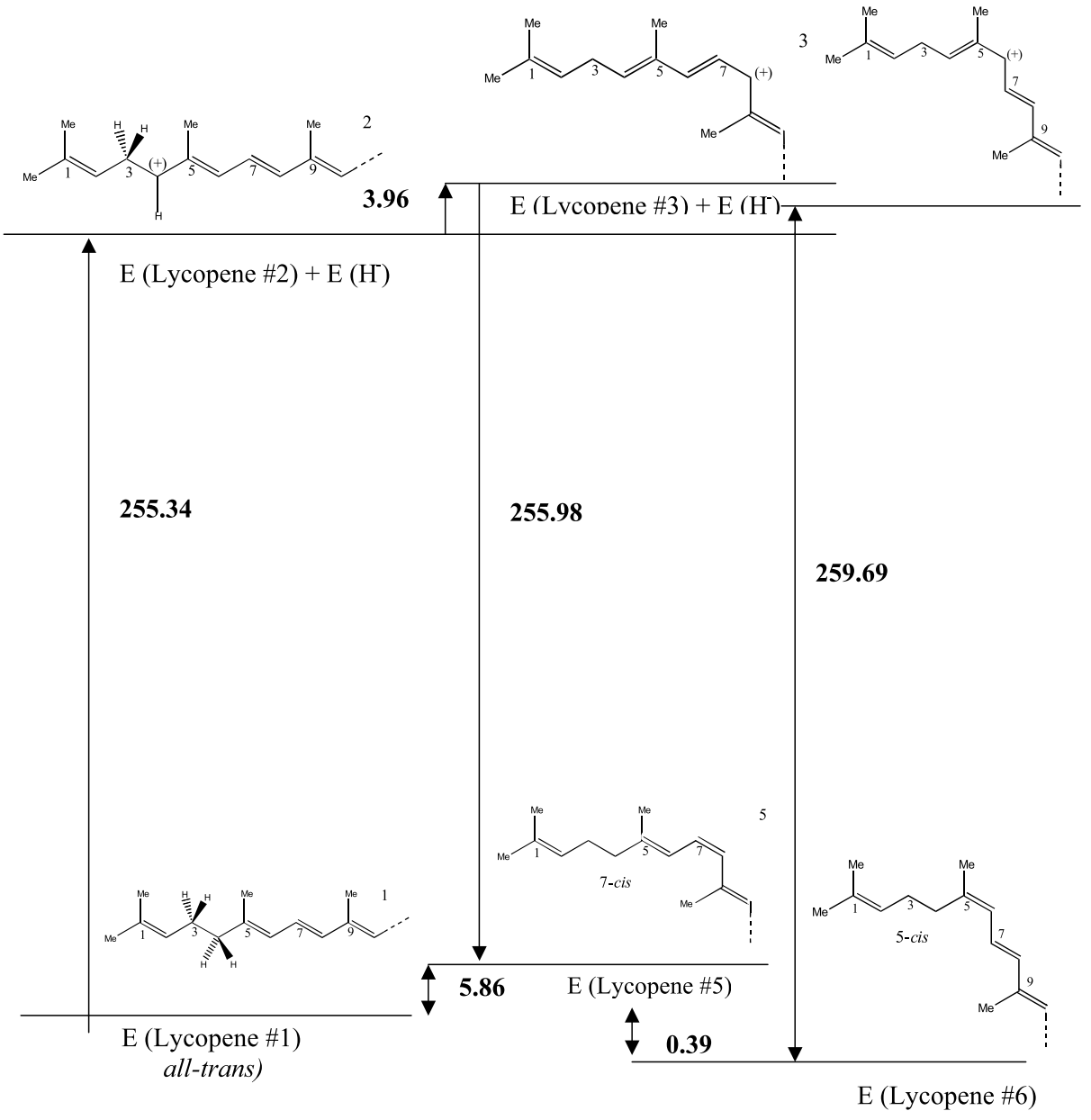

Fig. 13. Energy level diagram (kcal mol^{-1}) for *trans–cis* isomerization mechanism of the truncated lycopene model.

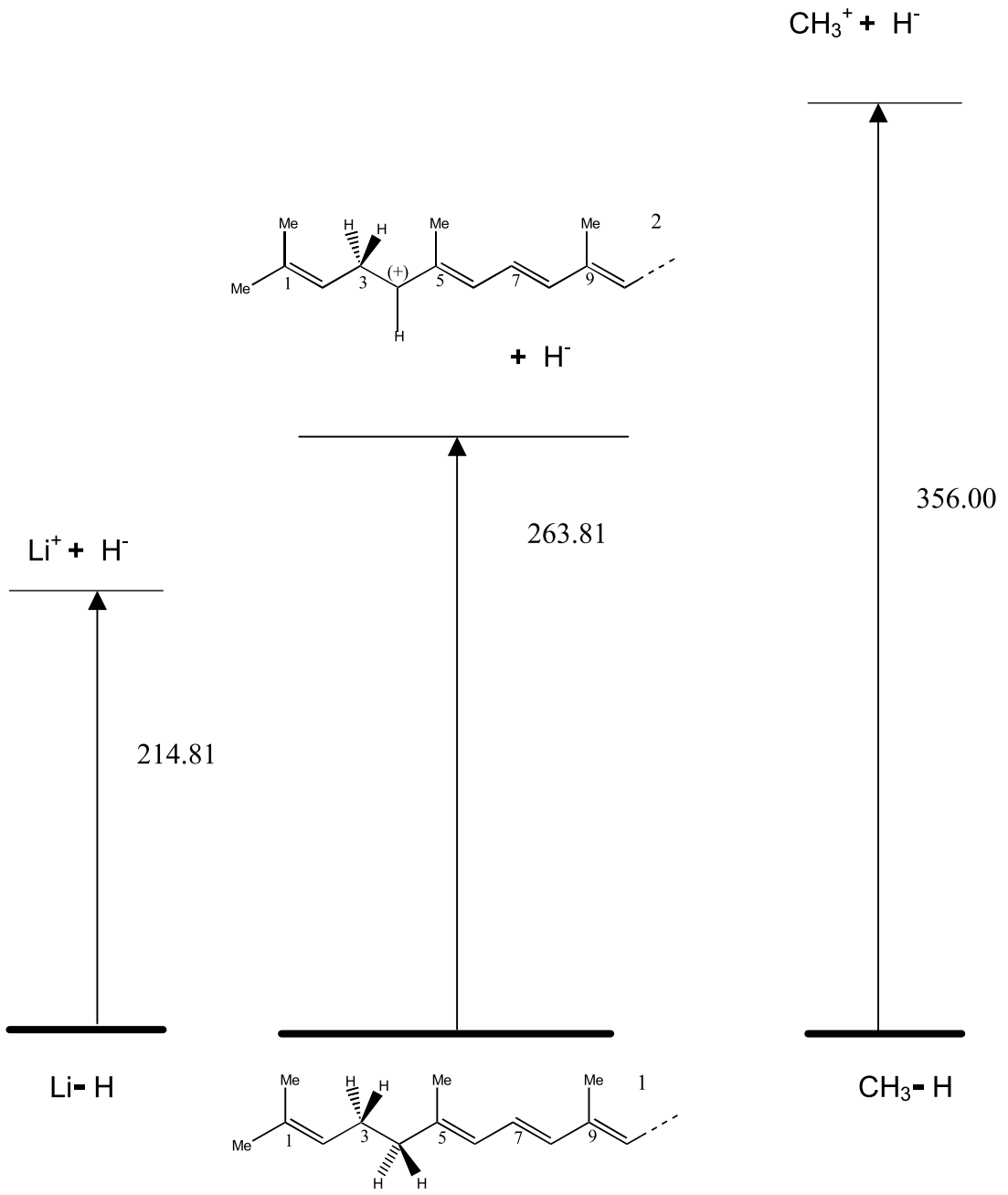

Fig. 14. Side-by-side comparison of hydride affinities (kcal mol^{-1}) for several small cationic systems.

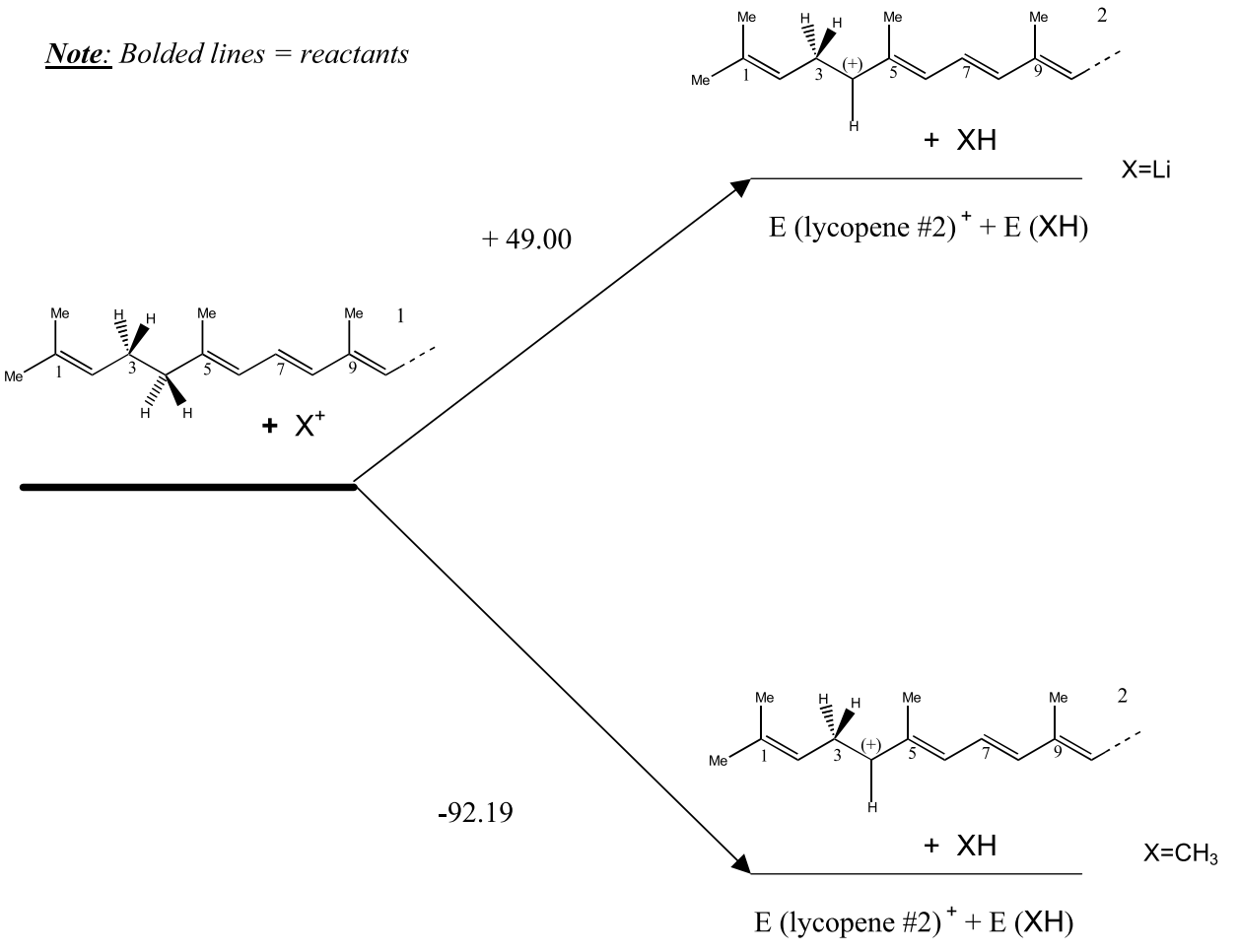

Fig. 15. Energy level diagram (kcal mol^{-1}) for hydride ion transfer from neutral all-*trans* lycopene Model C to selected cationic species.

Fig. 14 where a weak hydride acceptor [$Li^{(+)}$] is compared to a strong hydride acceptor [$H_3C^{(+)}$], as summarized in Table 4. The overall reaction may be endothermic for a weak hydride acceptor [$Li^{(+)}$], or exothermic for a strong hydride acceptor [$H_3C^{(+)}$], as shown in Fig. 15.

No attempt is made here to study $NAD^{(+)}$, because it is believed that the hydride affinity of $NAD^{(+)}$ is not just the hydride affinity of the pyridinium ring. It is quite likely modified by the carbohydrate attached, as well as by the remaider of the $NAD^{(+)}$ molecule.

5. Conclusions

All of the results obtained suggest that the isomerization mechanism proposed is indeed plausible.

The following sequence of stability is observed:

5-*cis* > all-*trans* > 7-*cis*

for the neutral tail-end (C_1–C_{10})model of lycopene (Model C).This is in line with the results from previous studies [11] on the various isomers of the entire lycopene. The relative stability of the intermediate cations generated from Model C, however exhibited a different stability:

all-*trans* > 5-*cis* > 7-*cis*.

Acknowledgements

The authors are grateful to Professor A. Kucsman for helpful discussions. We also wish to thank Keneth P. Chasse (math@velocet.ca), Graydon Hoare (graydon@pobox.com)and Velocet Communications Inc. for database management, network support, software and distributive processing development. A special thanks is also extended to Andrew M. Chasse (fixy@fixy.org) for his continuing and ongoing development of novel scripting and coding techniques, helping to bring about a reduction in the necessary number of CPU cycles for each computation.

References

[1] F. Khachik, J.S. Bertram, M.T. Huang, J.W. Fahey, P. Talalay, in: L. Packer (Ed.), Antioxidant Food Supplements in Human Health, Academic Press, New York, 1999, pp. 203–228.
[2] D. DellaPenna, J. Pure Appl. Chem. 71 (1999) 2205–2212.
[3] M. Paolini, G. Cantelli-Forti, P. Perocco, G.F. Pedulli, S.Z. Abdel-Rahman, M.S. Legator, Nature 398 (1999) 760–761.
[4] P.M. Bramley, Phytochemistry 54 (2000) 233–236.
[5] W. Stahl, H. Sies, in: L. Packer (Ed.), Antioxidant Food Supplements in Human Health, 1999, pp. 183–202.
[6] H. Sies, W. Stahl, Proc. Soc. Exp. Biol. Med. 218 (1998) 121–124.
[7] H. Sies, W. Stahl, in: Ozben (Ed.), Free Radicals, Oxidative Stress, and Antioxidants, Plenum Press, New York, 1998, pp. 315–322.
[8] A.V. Rao, S. Agarwal, Nutr. Res. 19 (1999) 305–323.
[9] L. Zechmeister, R.B. Escue, J. Am. Chem. Soc. 66 (1944) 322–330.
[10] L. Pauling, Fortschr. Chem. Organ. Naturstoffe 3 (1939) 203–235.
[11] G.A. Chasse, K.P. Chasse, A. Kucsman, L.L. Torday, J.G. Papp, Theochem (2001) (in press).
[12] M.J. Frisch, G.W. Trucks, H.B. Schlegel, P.M.W. Gill, B.G. Johnson, M.A. Robb, J.R. Cheeseman, T. Keith, G.A. Petersson, J.A. Montgomery, K. Raghavachari, M.A. Al-Laham, V.G. Zakrzewski, J.V. Ortiz, J.B. Foresman, J. Cioslowski, B.B. Stefanov, A. Nanayakkara, M. Challacombe, C.Y. Peng, P.Y. Ayala, W. Chen, M.W. Wong, J.L. Andres, E.S. Replogle, R. Gomperts, R.L. Martin, D.J. Fox, J.S. Binkley, D.J. Defrees, J. Baker, J.P. Stewart, M. Head-Gordon, C. Gonzalez, J.A. Pople, GAUSSIAN 94, Revision E.2, Gaussian, Inc., Pittsburgh PA, 1995.